Reduction of self-phase modulation in double-clad photonic crystal fiber for nonlinear optical endoscopy

Hongchun Bao and Min Gu*

Centre for Micro-Photonics, Faculty of Engineering and Industrial Sciences, Swinburne University of Technology, Hawthorn, Victoria 3122, Australia
*Corresponding author: mgu@swin.edu.au

Double-clad photonic crystal fiber and double-clad fiber have been widely used in multiphoton-excited fluorescence or second-harmonic generation (SHG) endoscopy. We provide a useful comparison of two fibers used in nonlinear optical microendoscopy. While a double-clad fiber is found to have a higher percentage of the output power from its core, which results in the efficient utilization of the power of the excitation laser, a double-clad photonic crystal fiber has a higher threshold of the nonlinearity, which effectively reduces the self-modulation effect and thus leads to a higher degree of polarization of the excitation beam. Consequently, the use of the double-clad photonic crystal fiber facilitates bright two-photon fluorescence imaging as well as polarized SHG imaging. © 2009 Optical Society of America

OCIS codes: 180.4315, 170.2150, 110.2350, 190.4370.

Two-photon fluorescence microscopy with reduced phototoxicity compared with single-photon imaging has become an indispensable tool for high-resolution imaging of biological cells within tissue, which are too deep to access by conventional microscopy [1–3]. A great interest is in the imaging capability permitting the structure and organization of individual cells inside living subjects to be studied and visualized *in vivo* without biopsy [4,5]. However a benchtop nonlinear optical microscope for two-photon fluorescence and second-harmonic generation (SHG) imaging is difficult for *in vivo* imaging, because it cannot be moved flexibly around and does not have a small-size probe.

Nonlinear optical endoscopy uses an optical fiber with a miniaturized probe, where the probe can move flexibly around for *in vivo* imaging and for imaging interorgans *in vivo* [5–10]. Recently a double-clad fiber (DCF) has been used in endoscopy and multiphoton fluorescence endoscopy [11–13]. The DCF has the same size as a standard single-mode fiber and a solid core and inner- and outer-clad regions. It has been proved to be robust and cost effective to be used in the probe with a microscanner scanning the optical fiber [11,12,14]. Alternatively, double-clad photonic crystal fiber (DCPCF) has also been adopted in nonlinear optical endoscopies [15–19]. The DCPCF has a large core size and a high NA, which leads to a high signal collection for nonlinear optical microendoscopy. In this Letter, we demonstrate that the comparison of the DCPCF and the DCF for nonlinear microendoscopy exhibits a low nonlinearity owing to the reduction of the self-modulation effect in the former.

A schematic setup for comparing the performance between a DCPCF (Crystal Fibre, DC-165-16-Passive) and a DCF (Fibercore Ltd, SMM900) is displayed in Fig. 1. The insert of Fig. 1 shows the structure of the DCPCF and the DCF. The DCPCF has 16, 135, and 350 μm core, inner-, and outer-clad diameters, respectively, while the DCF has 3.6, 105, and

125 μm core, inner-, and outer-clad diameters, respectively [11–19]. 70 fs short pulses with a repetition rate of 80 MHz generated from a Ti:sapphire laser are prechirped by a grating pair to compensate for chromatic dispersion of fibers and coupled into a 3 m DCPCF or a DCF by a lens (L_1). Here an Olympus MA20 NA 0.4 objective lens is used for coupling the excitation laser into the DCF, where the pulsed laser beam underfills the objective lens and the effective NA of the laser beam to the DCF is 0.2, matching the core NA of the DCF. On the other hand, a single lens with a focal length of 100 mm is employed for coupling the excitation pulses into the DCPCF so that the NA of the beam into the PCF is 0.04—agreeing with the core NA of the DCPCF. The output from the fiber is collimated by the same lens as L_1. In both cases, the beam size is kept the same, which results in the same NA on a sample throughout the experiment. The collimated beam is focused onto a sample by an objective lens (Olympus UplanApo 40 $\times$/0.85). Nonlinear signals generated from the sample are collected by the objective lens, passed through the fiber, separated from the excitation laser beam by a dichroic mirror, and then sent to a photomultiplier tube (PMT). Two-photon fluorescence im-
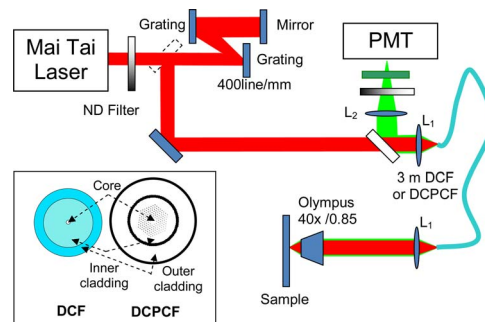

Fig. 1.   (Color online) Schematic setup in nonlinear optical microendoscopy using a 3 m DCF or a 3 m DCPCF. Inset, structure of the DCF and the DCPCF.

ages and SHG images are achieved by placing a 3-mm-thick BG18 glass filter (Schott Pty Ltd.) and a 400/9 nm bandpass filter before the PMT, respectively. The distance between the grating pair is optimized for achieving the maximum nonlinear signal.

As the NA of the excitation laser beam matches that of the core of the DCPCF and the DCF, the corresponding coupling efficiencies are 82% and 91%, respectively. However, among total output power from the fiber, 38% and 70% come from the core in the former and latter cases, respectively, where the power from the core of the fiber was measured by using a pinhole with the size matching the core diameter of the DCPCF and the DCF to block the laser from the inner cladding region of the fiber. The laser beam from the core of the fibers is a single-mode beam and has the chromatic dispersion that can be compensated for by the prechirp unit. The rest of the laser beam comes from the light propagating through the inner-clad region of the fiber and has multiple modes, where the large modal dispersion cannot be compensated. The nonlinear signal generated by the laser beam from the inner clad of the fiber is much weaker than that from the core of the fiber and thus can be ignored. The DCF has a high percentage of output laser from the core of the fiber for generating a nonlinear signal. In that sense, the DCF can more efficiently transmit the excitation laser power for nonlinear imaging.

However, the DCF results in a stronger nonlinearity and the degradation of the polarization of the laser beam owing to its smaller core size. Figure 2(a) shows the log–log dependence of the two-photon fluorescence intensity versus the output power from their core in the cases of the DCPCF and the DCF, where the two-photon fluorescence intensity was measured from the sample before it enters to the fiber. The dependence in the case of the DCPCF is linear up to the core power of 50 mW. However, this dependence in the case of the DCF is linear only up to the core power of 15 mW. In both cases, the gradient of the linear relations show a slope of 1.8, close to 2. As the power from the core of the DCF is over 15 mW, the dependence is deviated from the linear relation. This deviation is caused by the nonlinear effect such as the self-phase modulation, resulting in the broadening of the laser pulses within the fiber [20–22] and
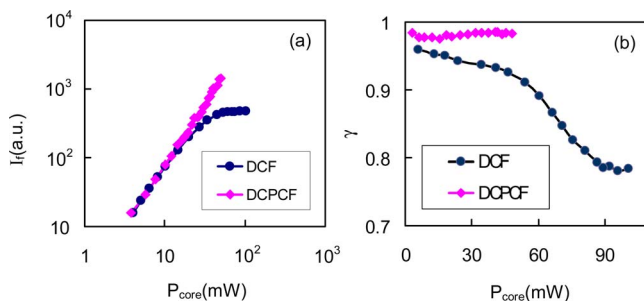
the reduction of the two-photon fluorescence signal from the sample. The core diameters of the DCF and the DCPCF are 3.6 and 16 μm, respectively. If the powers from the core of the DCF and the DCPCF are the same, the power intensity in the DCPCF is only about 1/20 of that in the DCF. The nonlinearity in the DCPCF is much smaller than that in the DCF.

Another outcome of the stronger self-phase modulation in the DCF is the reduction of the degree of polarization of the excitation beam on the sample. The degree of polarization, defined as $\gamma = (I_{max} - I_{min})/(I_{max} + I_{min})$, where I_{max} and I_{min} are the maximum and minimum intensity of the output beam from the core of the fiber measured through a Glenn–Thompson polarizer analyzer, as a function of the core power is shown in Fig. 2(b). In the case of the DCPCF, γ is 0.98 up to the power of 50 mW. But for the DCF, it is 0.95 up to the core power of 18 mW and decreases with the increase of the power at a higher power level. γ is only 0.78 as the core power reaches 90 mW, which means that the use of the DCF degrades not only the two-photon fluorescence signal level but also the degree of polarization of the SHG signal.

Figure 3 shows the two-photon fluorescence images of 10 μm fluorescence microspheres by using the 3 m DCPCF and the 3 m DCF. When the core power from the fiber is 11 mW, the brightness of two-photon fluorescence images in both cases is almost the same, as shown in Figs. 3(a) and 3(d). As the core power increases to 21 mW, the two-photon fluorescence image using the DCPCF is brighter than that using the DCF, as displayed by Figs. 3(b) and 3(e). At this power, the DCF starts to show the nonlinear self-phase modulation, which leads to the reduction of two-photon fluorescence generation as indicated in Fig. 2(a). As the input power further increases to 185 mW, which corresponds to the core power of 48 and 100 mW in the cases of the DCPCF and the DCF. Although the core power in the DCF is approximately
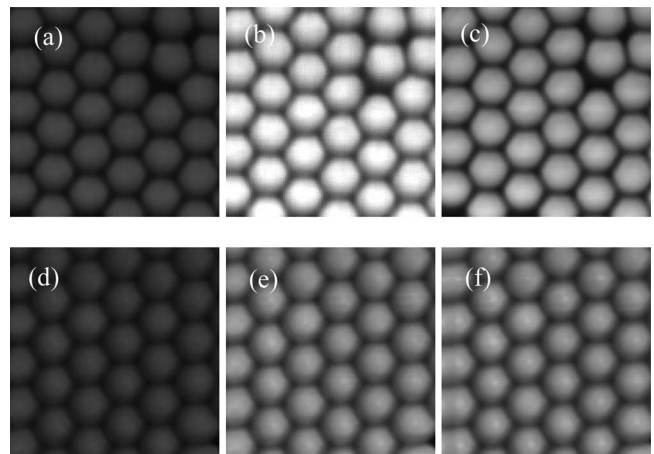
Fig. 3. Two-photon fluorescence images of 10 μm fluorescence microspheres excited by the output from the DCPCF as the core power is (a) 11, (b) 21, and (c) 48 mW with the 0.5 attenuation ND filter. The two-photon fluorescence images excited by the output from the DCF as the core power is (d) 11, (e) 21, and (f) 100 mW. The size of the images is 50 μm $\times$ 50 μm.

Fig. 2. (Color online) Log–log plot of the two-photon fluorescence intensity (I_f) versus the excitation laser power from the core of the fiber (P_{core}). (b) The degree of polarization γ of the output from the core of the DCF and the DCPCF as a function of the output power from their core.

two folds of that in the DCPCF, the two-photon fluorescence image in the latter is much brighter than that in the fomer and a neutral density (ND) filter with attenuation of 0.5 is needed in front of the PMT to keep the same brightness of the image, as indicated in Figs. 3(c) and 3(f).

Figure 4 shows the SHG images of β-bariumborate (BBO) microcrystals using the 3 m DCPCF and the 3 m DCF. At the core power of 16 mW, the SHG image using the DCPCF is slightly brighter than that using the DCF, as shown in Figs. 4(a) and 4(d), since the degree of polarization from the output of the DCPCF is a little higher than that of the DCF, as illustrated in Fig. 2(b). As the core power increases to 33 mW, the SHG image using the DCPCF is much brighter than that using the DCF, as displayed in Figs. 4(b) and 4(e). At this power, the nonlinear self-phase modulation in the DCF not only broadens the pulses, which reduces the SHG signal, but also degrades the degree of polarization. Those two factors cause the brightness of the SHG image using the DCF to be much less than that using the DCPCF. As the input power increases to 185 mW, the SHG image using the DCPCF with a ND filter with an attenuation of 0.5 and the SHG image using the DCF without the ND are displayed in Figs. 4(c) and 4(f), respectively.

In summary, both the DCPCF and the DCF can be used in nonlinear optical microendoscopy, where the core of the fiber is used for delivering the near-infrared excitation laser beam to the sample and the inner clad of the fiber can be adopted for collecting the visible signal for imaging. Although the percentage of the core power from the DCF is about twofolds larger than that from the DCPCF, the nonlinear self-phase modulation effect within the DCF is much stronger than that in the DCPCF owing to the smaller core size in the former. This in-fiber nonlin-

earity broadens the excitation laser pulses and degrades the degree of polarization of the excitation laser beam, which degrades the signal generation. Our experiment demonstrates that even the core power in the DCPCF is only half of that in the DCF when the input power is 185 mW, the two-photon fluorescence and SHG images using the DCPCF is threefolds as bright as that using the DCF.
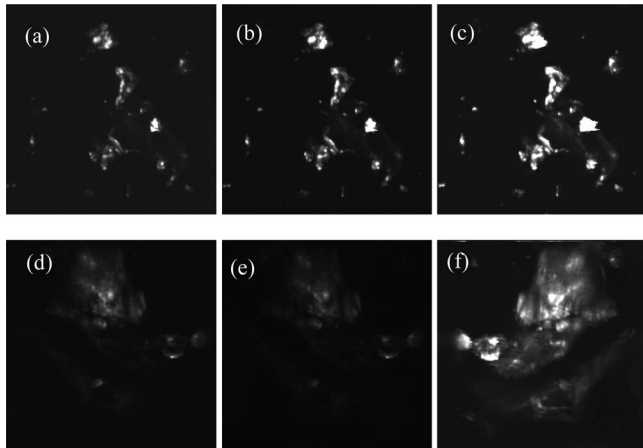
Fig. 4. SHG images of BBO microcrystals excited by the output from the DCPCF as the power in the core is (a) 16, (b) 33, and (c) 48 mW with a 0.5 attenuation ND filter. The SHG images excited by the output from the DCF as the core power is (d) 16, (e) 33, and (f) 100 mW. The size of the images is 100 μm $\times$ 100 μm.

References

1. W. Denk, J. H. Strickler, and W. W. Webb, Science **248**, 73 (1990).
2. F. Helmchen and W. Denk, Nat. Methods **2**, 932 (2005).
3. P. Theer, M. T. Hasan, and W. Denk, Opt. Lett. **28**, 1022 (2003).
4. J. C. Jung, A. D. Mehta, E. Aksay, R. Stepnoski, and M. J. Schnitzer, J. Neurophysiol. **92**, 3121 (2004).
5. K. Konig, A. Ethlers, I. Riemann, S. Schenkl, R. Buckle, and M. Kaatz, Microsc. Res. Tech. **70**, 398 (2007).
6. B. A. Flusberg, J. C. Jung, E. D. Cocker, E. P. Anderson, and M. J. Schnitzer, Opt. Lett. **30**, 2272 (2005).
7. C. J. Engelbrecht, R. S. Johnston, E. J. Seibel, and F. Helmchen, Opt. Express **16**, 5556 (2008).
8. T. P. Thomas, M. T. Myaing, J. Y. Ye, K. Candido, A. Kotlyar, James Beals, P. Cao, B. Keszler, A. K. Patri, T. B. Norris, and J. R. Baker, Jr., Biophys. J. **86**, 3959 (2004).
9. B. A. Flusberg, E. D. Cocker, W. Piyawattanametha, J. C. Jung, E. L. M. Cheung, and M. J. Schnitzer, Nat. Methods **2**, 941 (2005).
10. D.. Bird and M. Gu, Opt. Lett. **28**, 1552 (2003).
11. M. T. Myaing, D. J. MacDonald, and X. Li, Opt. Lett. **31**, 1076 (2006).
12. H. Bao, J. Allen, R. Pattie, R. Vance, and M. Gu, Opt. Lett. **33**, 1333 (2008).
13. D. Yelin, B. E. Bouma, S. H. Yun, and G. J. Tearney, Opt. Lett. **29**, 2408 (2004).
14. M. Goetz, C. Fottner, E. Schirrmacher, P. Delaney, S. Gregor, C. Schneider, D. Strand, S. Kanzler, B. Memadathil, E. Weyand, M. Holtmann, R. Schirrmacher, M. M. Weber, M. Anlauf, G. Klöppel, M. Vieth, P. R. Galle, P. Bartenstein, M. F. Neurath, and R. Kiesslich, Endoscopy **39**, 350 (2007).
15. M. T. Myaing, J. Y. Ye, T. B. Norris, T. Thomas, J. R. Baker, W. J. Wadsworth, G. Bouwmans, J. C. Knight, and P. St. J. Russell, Opt. Lett. **28**, 1224 (2003).
16. L. Fu and M. Gu, Opt. Lett. **31**, 1471 (2006).
17. L. Fu, A. Jain, H. Xie, C. Cranfield, and M. Gu, Opt. Express **14**, 1027 (2006).
18. L. Fu and M. Gu, Opt. Express **16**, 5000 (2008).
19. L. Fu, A. Jain, C. Cranfield, H. Xie, and M. Gu, J. Biomed. Opt. **12**, 040501 (2007).
20. G. P. Agrawal, *Nonlinear Fiber Optics*, 2nd ed. (Academic, 1995).
21. D. G. Ouzounov, K. D. Moll, M. A. Foster, W. R. Zipfel, W. W. Webb, and A. L. Gaeta, Opt. Lett. **27**, 1513 (2002).
22. F. Helmchen, D. W. Tank, and W. Denk, Appl. Opt. **41**, 2930 (2002).